Phys. Status Solidi RRL **6**, No. 5, 193–195 (2012) / **DOI** 10.1002/pssr.201206030

pss +++rapid research letters+++
www.pss-rapid.com

Silicon heterojunction solar cell with amorphous silicon oxide buffer and microcrystalline silicon oxide contact layers

Kaining Ding*, **Urs Aeberhard, Friedhelm Finger, and Uwe Rau**

IEK-5 Photovoltaik, Forschungszentrum Jülich, Leo-Brandt-Straße, 52425 Jülich, Germany

Received 24 January 2012, revised 9 March 2012, accepted 9 March 2012
Published online 13 March 2012

Keywords silicon, solar cells, buffer layer, interfaces, passivation, PECVD

* Corresponding author: e-mail k.ding@fz-juelich.de, Phone: +492461611604, Fax: +492461613735

This Letter reports on the fabrication and characterization of silicon heterojunction solar cells with silicon oxide based buffer (intrinsic amorphous silicon oxide) and contact layers (doped microcrystalline silicon oxide) on flat p-type wafers. The critical dependency of the cell performance on the front and rear buffer layer thickness reveals a trade-off between the open circuit voltage V_{oc} and the fill factor FF. At the optimum, the highest efficiency of 18.5% (active area = 0.67 cm^2) was achieved with V_{oc} = 664 mV, short circuit current J_{sc} = 35.7 mA/cm^2 and FF = 78.0%.

1 Introduction Solar energy conversion efficiencies of 23% have been demonstrated for silicon heterojunction (SHJ) solar cells using intrinsic amorphous silicon (a-Si:H) as buffer layer material and n/p doped amorphous silicon as contact layer materials [1]. Doped microcrystalline silicon oxide (μc-SiO$_x$:H), consisting of a phase mixture of silicon crystallites and amorphous silicon oxide tissue, is used in silicon thin-film solar cells as intermediate reflector [2] or wide gap window layer [3] due to its beneficial optical properties (high optical band gap, favourable refractive index). Partial implementation of this material as emitter or back contact material in SHJ solar cells has also been reported [4, 5]. Intrinsic amorphous silicon oxide (a-SiO$_x$:H) was shown to have excellent passivation properties [6] and, as compared to a-Si:H, a higher optical band gap and suppression of epitaxial growth [7]. However, up to the present no silicon heterojunction solar cell has been reported involving all buffer layers made from a-SiO$_x$:H and all contact layers made from μc-SiO$_x$:H materials.

In this work, we demonstrate the potential of SHJ solar cells with full silicon oxide based buffer and contact layers on p-type wafer using μc-SiO$_x$:H ⟨n⟩ as emitter, μc-SiO$_x$:H ⟨p$^+$⟩ as back surface field (BSF) and a-SiO$_x$:H ⟨i⟩ as buffer layer for both contacts. In particular, we investigated the critical dependency of the cell performance on the buffer layer thickness.

2 Experimental Figure 1 sketches the structure of the silicon heterojunction (SHJ) solar cell. As absorber material, we used double side polished, ⟨100⟩ orientated, 250 μm thick p-type float zone silicon wafers with a doping concentration of $4.62 \pm 0.15 \times 10^{15}$ cm^{-3} determined using capacitance–voltage measurements on the SHJ solar cells. Prior to deposition, the wafers were treated in a mixture of sulphuric acid and hydrogen peroxide to clean off organic residues, followed by a dipping in diluted hydrofluoric acid to remove the native oxide from the wafer surface. The a-SiO$_x$:H ⟨i⟩, μc-SiO$_x$:H ⟨n⟩ and μc-SiO$_x$:H ⟨p$^+$⟩ layers were deposited using plasma enhanced chemical vapour deposition (PECVD) at 200 °C substrate temperature. We used SiH_4, CO_2, H_2 as process gases and PH_3, $B(CH_3)_3$ as doping gases. Details on the deposition parameters will be published elsewhere. The oxygen content of the a-SiO$_x$:H ⟨i⟩ buffer layer was 5% according to Rutherford backscattering spectrometry results. The cell is finished with sputtered indium tin oxide (ITO) on both sides, thermally evaporated silver grids through a shadow mask (active area = 0.67 cm^2) on the front side and full area silver on the rear side. As a final step, the cells were annealed on a heating plate at 200 °C for 2 min for contact forming and the improvement of passivation quality. In this study, only the thicknesses of the front and rear a-SiO$_x$:H ⟨i⟩ layers were varied between different cells. The thicknesses

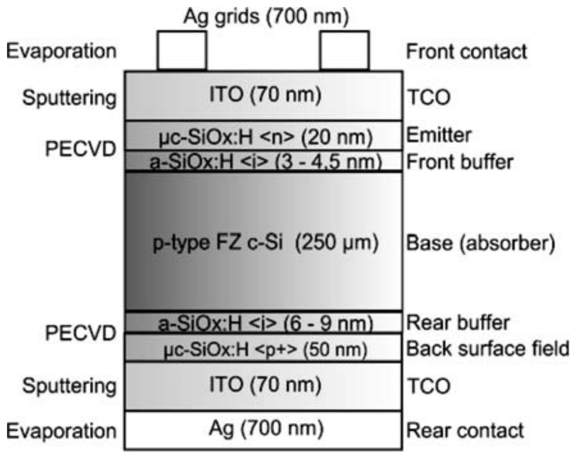

Figure 1 Schematic illustration of the SHJ solar cell structure with PECVD grown emitter, BSF and buffer layers on a flat p-type wafer covered with sputtered TCO and thermal evaporated silver.

were estimated from deposition times and the predetermined deposition rate.

A double source (Class A) AM1.5 solar simulator was used to determine the cell efficiencies η at standard test conditions (AM1.5G, 100 mW/cm^2, 25 °C), as well as fill factors FF, open circuit voltages V_{oc} and short circuit current densities J_{sc}. The external quantum efficiency (EQE) was measured in a differential spectral response (DSR) setup by positioning a focused light spot between two silver grids. The integrated short circuit current density $J_{sc,int}$ was determined by integrating the product of EQE and the AM1.5G solar spectrum over the wavelength range from 300 nm to 1150 nm. Considering $J_{sc,int}$ from DSR being more accurate than J_{sc} from the solar simulator, we recalculated the efficiency η_{act} of the active area from FF, V_{oc} and $J_{sc,int}$.

3 Results Figure 2 displays the solar cell parameters plotted versus the thickness of the a-SiO$_x$:H ⟨i⟩ rear buffer layer. The front buffer layer thickness was always kept at half the size of that of the rear buffer layer thickness. With increasing thickness of the rear buffer layer from 6.5 nm to 9.0 nm, the V_{oc} values increase linearly from around 630 mV to almost 680 mV. A small linear increase of $J_{sc,int}$ is also observable. However, the fill factor, first remaining at a high value of around 78% showing only slight deterioration with thickness, decreases strongly to 61% from 8.0 nm to 9.0 nm rear buffer thickness. Thus, η_{act} first increases with increasing buffer layer thickness due to the increase in V_{oc} and $J_{sc,int}$, while FF is still high. With further increase of the rear buffer layer thickness beyond 8.0 nm, η_{act} decreases due to significant loss in FF. The highest efficiency was obtained for the 8.0 nm cell with V_{oc} = 664 mV, $J_{sc,int}$ = 35.7 mA/cm^2, FF = 78.0% and η_{act} = 18.5%.

Figure 3 shows the EQE of three characteristic cells with different buffer layer thicknesses measured at the bias

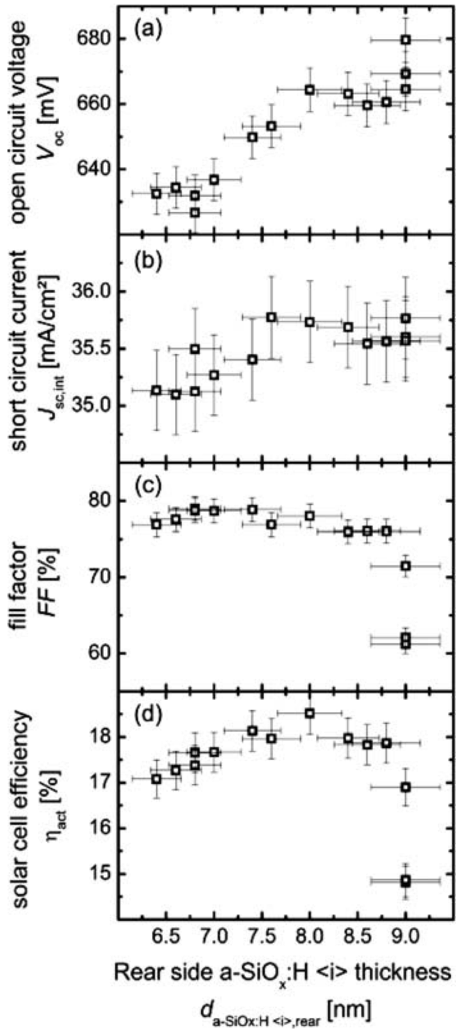

Figure 2 Dependence of the SHJ solar cell parameters on the thickness of the rear a-SiO$_x$:H ⟨i⟩ buffer layer. The front buffer layer thickness is always half that of the rear buffer layer thickness. A maximum effective area efficiency of 18.5% was achieved with V_{oc} = 664 mV, J_{sc} = 35.7 mA/cm^2 and FF = 78.0%.

voltage of 0 V. The cells achieved the highest EQE value of (98.7 ± 1.0)% at a wavelength around 630 nm. This surprisingly high EQE at the wavelength of 630 nm is verified by optical spectroscopy measurements on ITO layers deposited on glass substrates showing an absorptance of less than 0.05% and on SHJ solar cells showing a cell reflectance of 1.3%. With increasing buffer layer thickness, the EQE at long wavelengths increases, whereas the EQE in the short wavelength range decreases. However, the current gain at long wavelengths exceeds the current loss at short wavelength, giving rise to a total gain in $J_{sc,int}$ with increasing buffer layer thickness (Fig. 2b).

4 Discussion We fabricated SHJ solar cells using full silicon oxide based buffer, emitter and BSF layers on p-type wafer with a maximum efficiency of 18.5%. The high short circuit current density ($J_{sc,int}$ = 35.7 mA/cm^2) on a flat

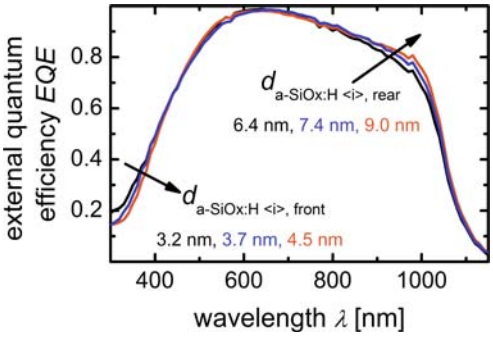

Figure 3 (online colour at: www.pss-rapid.com) External quantum efficiency of the SHJ solar cells with different front and rear a-SiO_x:H ⟨i⟩ buffer layer thicknesses measured at the bias voltage of 0 V. The increase (decrease) of EQE at long (short) wavelengths can be attributed to the increase of the rear (front) buffer layer thickness.

silicon wafer combined with a good fill factor (FF = 78.0%) demonstrates the potential of silicon oxide based thin layers as both optically and electrically promising layers in SHJ solar cells. The high open circuit voltage (V_{oc} = 664 mV) on p-type wafer confirms the good passivation quality of intrinsic amorphous silicon oxide. We showed that the cell performance strongly depends on the thickness of the buffer layers despite of only minute thickness variations.

The increase of EQE at long wavelengths with thicker buffer layers is due to improved carrier extraction and not due to a reduction of cell reflectance, since we have checked that the total reflectance of the cells does not change with small variations of the buffer layer thicknesses (not shown here). The increase of the carrier extraction at longer wavelengths implies that the passivation quality of the c-Si/a-SiO_x:H rear interface was improved with thicker buffer layer due to reduced recombination losses at the rear interface. We presume that a thicker rear buffer layer reduces the probability of electrons to tunnel through the buffer layer and recombine with holes via defect states at the a-SiO_x:H/μc-SiO_x:H interface. The decrease of EQE at short wavelengths likely originates from higher parasitic absorption in the front buffer layer with increasing thickness, since the EQE is sensitive to the thickness of thin layers at the front side [8]. Even though a possible increase of the carrier extraction at short wavelengths with thicker buffer layer is not observed, we cannot exclude an improvement of the passivation quality of the c-Si/a-SiO_x:H front interface with thicker buffer layer. The potential gain in current due to reduced recombination losses at the front interface might be overcompensated by the optical loss.

The variation of the FF with buffer layer thickness is largely related to the variation of the series resistance R_s of the cells. For thicker rear buffer layers, the dramatic decrease of the FF might result from the increase of the tunnelling resistance [9], which grows exponentially with the thickness of the intrinsic buffer layer. At smaller rear buffer layer thickness, the FF remains high despite of increasing buffer layer thicknesses, which is an indication for the limitation of the FF by other sources of series resistance, e.g. the Ag/ITO, ITO/μc-SiO_x:H contact resistances or the series resistance of the ITO or the μc-SiO_x:H layers.

Depending on the thickness of the buffer layers, there always seems to be a trade-off between FF and V_{oc}. The front buffer layer should be thin to guarantee low series resistance and low parasitic absorption. However, for a very thin front buffer layer and a reasonably thick rear buffer layer, front interface recombination might become the limiting factor for the V_{oc} and deteriorate the J_{sc} again. With a thicker rear buffer layer, the improved passivation quality at the rear interface results in higher V_{oc} and J_{sc}. However, if the rear buffer layer is too thick, the loss in FF will prevail over the gain in V_{oc} and J_{sc}. On textured wafers, the current collection will likely increase due to enhanced light trapping. With proper surface texturing, smoothing and wet-chemical oxidation prior to deposition, we might be able to maintain the good passivation quality of the a-SiO_x:H ⟨i⟩ layers on textured wafers resulting in comparable or higher V_{oc} than on flat wafers.

5 Conclusion We have successfully fabricated SHJ solar cells with a-SiO_x:H buffer layers and μc-SiO_x:H contact layers on flat p-type wafers. With increasing buffer layer thickness, the heterojunction interfaces are better passivated, leading to a higher V_{oc}, whereas the tunneling resistance of the buffer layer increases, resulting in a lower FF. At the optimum trade-off between FF and V_{oc}, a maximum effective area efficiency of 18.5% was achieved with V_{oc} = 664 mV, J_{sc} = 35.7 mA/cm^2 and FF = 78.0%.

Acknowledgements The authors gratefully acknowledge A. Doumit and J. Hotovy for ITO sputtering, W. Reetz for helping with the DSR measurements, and A. Lambertz for fruitful discussions on deposition of microcrystalline silicon oxide. Financial support was provided by the German Federal Ministry of Education and Research (BMBF) under Grant No. 03SF0352E.

References

[1] T. Mishima, M. Taguchi, and E. Maruyama, Sol. Energy Mater. Sol. Cells **95**, 18 (2011).

[2] A. Lambertz, T. Grundler, and F. Finger, J. Appl. Phys. **109**, 113109 (2011).

[3] V. Smirnov, W. Böttler, A. Lambertz, H. Wang, R. Carius, and F. Finger, Phys. Status Solidi C **7**, 1053 (2010).

[4] C. Banerjee, J. Sritharathikhun, A. Yamada, and M. Konagai, J. Phys. D **41**, 185107 (2008).

[5] S. Rattanapan, T. Watahiki, M. Miyajima, and M. Konagai, J. Phys. D **50**, 082301 (2011).

[6] T. Mueller, S. Schwertheim, M. Scherff, and W. R. Fahrner, Appl. Phys. Lett. **92**, 033504 (2008).

[7] H. Fujiwara, T. Kaneko, and M. Kondo, Appl. Phys. Lett. **91**, 133508 (2007).

[8] K. Ding, T. Kirchartz, B. E. Pieters, C. Ulbrich, A. M. Ermes, S. Schicho, A. Lambertz, R. Carius, and U. Rau, Sol. Energy Mater. Sol. Cells **95**, 3318 (2011).

[9] F. Einsele, P. J. Rostan, M. B. Schubert, and U. Rau, J. Appl. Phys. **102**, 094507 (2007).